

Preparation of Gold Nanoparticles Protected by a Cubic Silsesquioxane and Their Monolayer Formation on a Glass Substrate

Kensuke Naka,* Hideaki Itoh, and Yoshiki Chujo*

Department of Polymer Chemistry, Graduate School of Engineering, Kyoto University, Katsura, Nishikyo-ku, Kyoto 615-8510

Received December 22, 2003; E-mail: ken@chujo.synchem.kyoto-u.ac.jp

Gold nanoparticles were prepared via reduction of HAuCl_4 in the presence of octa(3-aminopropyl)octasilsesquioxane octahydrochloride (**1**) as a cubic linker. The cubic silsesquioxane **1** would stabilize the gold nanoparticles in addition to providing the amino-functionalized surface of the gold nanoparticles, which allows some chemical modification of their shells. We describe their monolayer formation on a glass substrate without any modification by electrostatic interaction.

Nanometer-scaled metal particles are theoretically predicted to exhibit quantized properties and to have various interesting properties compared with bulk metals, so they hold promise as advanced materials with new electronic, magnetic, and optic properties.¹ Many research studies have been conducted aimed at the realization of future nanomaterials. Efforts to build and pattern the metal nanoparticles into organized structures are playing a more important role to produce nanodevices with useful properties.² Development of simple methods for the fabrication of controlled organized structures is indispensable. Especially, the assembly of metal nanoparticles on solid supports has attracted substantial research efforts as a consequence of their unique electronic and optical properties.³ For example, colloidal gold and silver nanoparticles are excellent building blocks for surface enhanced Raman scattering-active substrates.⁴ Different techniques, including Langmuir–Blodgett technique and electrophoretic deposition technique,⁵ have been used to obtain two-dimensional assembling of metal nanoparticles. One of the efficient methodologies for the organization involves the utilization of electrostatic interaction between a substrate and metal nanoparticles.⁶ Schmitt et al. reported layered nanocomposite films prepared from colloidal metal nanoparticles through electrostatic interaction. The most successful routes required the surface modification of a solid substrate by positively charged polyelectrolytes because of the negatively charged metal nanoparticles.

Recently, we have reported an assembling of metal nanoparticles into spherical aggregates via self-organized spherical templates in a solution by using octa(3-aminopropyl)octasilsesquioxane octahydrochloride (**1**) as a cubic linker (Chart 1).⁷ Due to its cubic structure, the combination of **1** and metal ions in solution formed a stable and spherical colloid, which acted as a template for the formation of the spherical aggregate of metal nanoparticles. Here, we report the preparation of gold nanoparticles by direct reduction of HAuCl_4 by NaBH_4 in the presence of **1**. The cubic silica core is rigid and completely defined and the eight organic functional groups are appended to the vertexes of the cube via spacer linkage. The eight func-

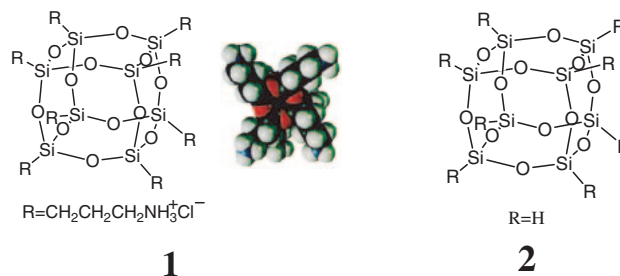


Chart 1.

tional groups of **1** are unable to attach to the same nanoparticle due to the steric hindrance of the cubic structure. The cubic silsesquioxane **1** would stabilize the gold nanoparticles in addition to providing the amino-functionalized surface of the gold nanoparticles, which allows some chemical modification of their shells. We also describe their monolayer formation on a glass substrate without any modification by electrostatic interaction.

Results and Discussion

Synthesis of Gold Nanoparticles. An excess amount of NaBH_4 (5 mg) was added dropwise to 10 mL of an aqueous solution of HAuCl_4 (2.4×10^{-3} M) in the presence of **1** (8.5×10^{-3} M). The solution color immediately changed from yellow to dark red, indicating the formation of gold nanoparticles. The obtained solution of the **1**-protected gold nanoparticles was stable without precipitation for several months. The UV–vis absorption spectrum of the dark-red solution of the **1**-protected gold nanoparticles showed the surface plasmon band at around 525 nm. TEM investigation showed the **1**-protected gold nanoparticles with an average diameter of 5.9 nm (Fig. 1). The **1**-protected gold nanoparticles were purified by dialysis using ultrafiltration to remove free **1** and the metal ions. Thermogravimetric analysis established that the percentage of **1** by weight in the gold nanoparticle was 4.0%. Based on the fact that the average particle size was 5.9 nm, the num-

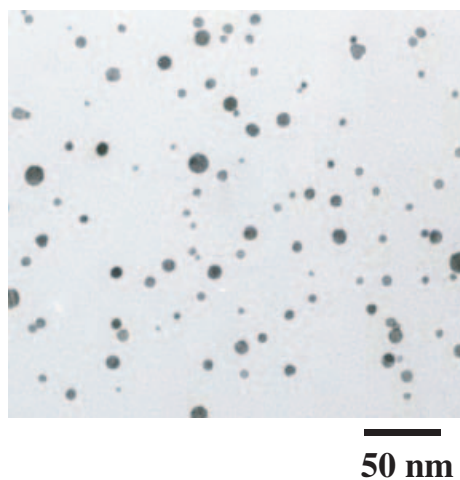


Fig. 1. TEM image of the **1**-protected gold nanoparticles.

ber of **1** molecules adsorbed on the surface of each nanoparticle was calculated to be 43. This value is lower than the theoretical value of 76 obtained from the assumption that **1** molecules densely adsorbed on the surface of the gold nanoparticles.

Two control experiments were carried out. When octahydrooctasilsesquioxane (**2**) was used instead of **1** under the same condition, insoluble black precipitates were observed. The stable colloidal form of the gold nanoparticles was not obtained. The difference between **1** and **2** was the presence of the functional group at the corner. These results indicate that the amino groups positioned at the corners of **1** attached on the surface of the gold.

The use of 1,8-diaminooctane dihydrochloride instead of **1** resulted in the formation of an insoluble black precipitate. This is due to the subsequent cross-linking reaction between the nanoparticles to form insoluble aggregates. This result is consistent with those in the previous paper.⁸ The utilization of organic dithiols as stabilizing ligands leads directly to the formation of an insoluble precipitate of dithiol cross-linked clusters of the gold nanoparticles. In contrast, the utilization of **1** molecules as stabilizing ligands resulted in the monodispersed gold nanoparticles as described above. The difference would be due to the cubic structure and multifunctionality. Unlike the bifunctional linking molecules, we expected stronger bonding of the cubic silsesquioxane to the metal nanoparticles due to a chelate effect, which prevents the growth of gold nanoparticles. The multifunctionality of **1** would provide the stronger electrostatic repulsive between the gold nanoparticles, which would prevent the subsequent cross-linking reaction. The details of the mechanism of growth of the gold nanoparticles are currently under investigation.

The dispersibility of the **1**-protected gold nanoparticles was strongly affected by solution pH. When the solution pH increased to around 8 with NaOH, a large red shift of the surface plasmon band was observed, indicating the aggregation of the **1**-protected gold nanoparticles. Since the amino groups of **1** were deprotonated around pH = 8 as measured by titration, we conclude that the aggregation of the **1**-protected gold nanoparticles is related to the change of the deprotonation of **1**. The

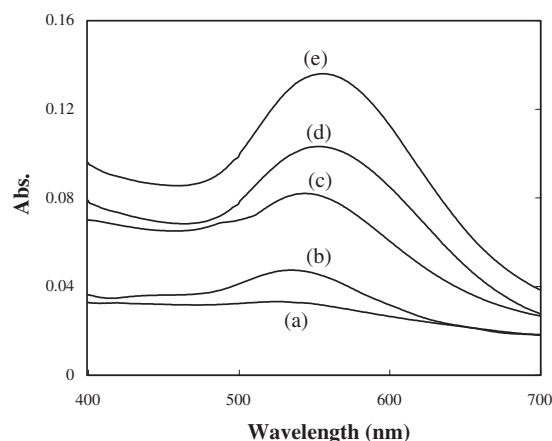


Fig. 2. UV-vis absorption spectra of the obtained glass substrate upon immersion in a solution after (a) 10 min, (b) 30 min, (c) 3 h, (d) 24 h, (e) 48 h.

evidence indicates that the amino groups locate on the outer surface of the gold nanoparticles due to the steric hindrance of **1**, which allows some chemical modification of their shells. At pH < 8, amino groups are dominantly positively charged, which promoted the dispersibility of the **1**-protected gold nanoparticles by strong electrostatic repulsion. At pH > 8, the deprotonation of the amino groups resulted in the decrease of the electrostatic repulsion, leading to the aggregation of the **1**-protected gold nanoparticles. Sastry et al. also reported some pH dependent changes in the optical properties of carboxylic acid derivatized silver colloidal particles.⁹ At low pH, considerable flocculation was observed due to the lack of coulombic stabilization.

Formation of Monolayer of Gold Nanoparticles. The adsorption of the **1**-protected gold nanoparticles on the glass substrate was monitored by UV-vis absorption spectra. Figure 2 shows visible optical spectra over time for the obtained glass substrate upon immersion in a solution. After 30 min, an absorbance feature at 537 nm indicated the adsorption of the **1**-protected gold nanoparticles. The absorbance continually increased with increasing the immersion time. The surface plasmon band gradually red-shifted from 525 nm to 566 nm. This is a consequence of overlap of the dipole resonances between neighboring gold nanoparticles on the glass substrate. That is, as the particle coverage increases, the interparticle spacing becomes small compared to the incident wavelength. These results indicate that the **1**-protected gold nanoparticles have a positive charge and were immobilized densely on the glass substrate.

Figure 3 shows the time course plots of the absorbance and the wavelength maximum of the **1**-protected gold nanoparticles on the glass substrate. The absorbance increases rapidly in the first 3 h but is then saturated. This phenomenon can be explained as follows. At the initial stage of immersion, electrostatic attraction between a negatively charged glass substrate and the positively charged **1**-protected gold nanoparticles in solution results in the rapid adsorption of the **1**-protected gold nanoparticles on the glass substrate. The increase of the particle coverage allows for charge reversal from negative to positive on the glass surface. The electrostatic repulsion of

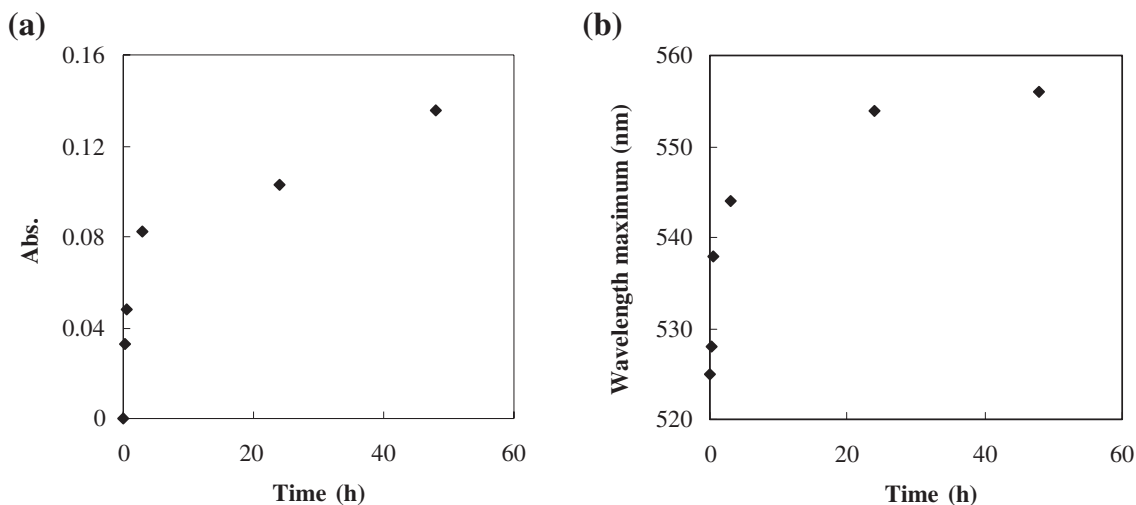


Fig. 3. (a) Absorbance versus time for the obtained glass substrate. (b) Wavelength maximum versus time for the obtained glass substrate.

equally charged gold nanoparticle results in the self-regulation of the adsorption. Therefore, the absorbance and red-shift in the UV-vis absorption spectrum become saturated. Yonezawa et al. also reported the saturation of the negatively charged gold nanoparticles' adsorption on the positively charged substrate.¹⁰

The effect of the concentration of the **1**-protected gold nanoparticles adsorbed on the glass was studied. The colloidal gold nanoparticles' solution was prepared with HAuCl_4 (0.8×10^{-3} M) and **1** (2.8×10^{-3} M) in the same way as described above. UV-vis absorption spectrum showed the similar adsorption behavior of the **1**-protected gold nanoparticles with HAuCl_4 concentration at 2.4×10^{-2} M as shown in Fig. 3. The surface plasmon band reached the maximum absorption after 48 h. These values are in good agreement with that of HAuCl_4 concentration at 2.4×10^{-2} M. If the multilayer and three-dimensional clusters of the **1**-protected gold nanoparticles were formed, higher absorbance would be expected under higher HAuCl_4 concentration condition. That is, UV-vis absorption spectrum indicates the formation of a monolayer of the gold nanoparticles in the present system. The uniform monolayer formation was confirmed by an atomic force microscopy (AFM) study (Fig. 4). The picture indicates that the film is very uniform with step heights consistent with the size of the **1**-protected gold nanoparticle.

The **1**-protected gold nanoparticles with a diameter of 80 nm were prepared at a HAuCl_4 /**1** molar ratio of 20. The glass substrate was immersed in this solution in the same way as describe above. Figure 5 shows the scanning electron microscopy (SEM) images for the obtained glass substrate. The light particles represent the **1**-protected gold nanoparticles. The SEM image indicates that the **1**-protected gold nanoparticles are homogeneously distributed and cover a wide area on the glass surface. No three-dimensional clusters of the **1**-protected gold nanoparticles were not present. The monolayer of the **1**-protected gold nanoparticles was formed due to the self-regulation of the adsorption. The monitor of the adsorption of the gold nanoparticles by SEM also showed an increase of the particle coverage with increasing the immersion time.

Conclusion

We have demonstrated that gold nanoparticles were successfully obtained by NaBH_4 reduction of HAuCl_4 in the presence of **1**. The obtained gold nanoparticles have amino-functionalized surfaces. The **1**-protected gold nanoparticles could be assembled effectively on the glass by electrostatic interaction. We confirmed separately that an alternate layer-by-layer assembly is possible in the present system.

Experimental

Materials. All solvents and reagents were obtained from commercial sources and used as supplied.

Measurement: ^1H NMR spectra were obtained with a JOEL JNM-EX270 spectrometer (270 MHz). UV-visible spectra were measured on a Jasco V-530 spectrometer. Transmission electron microscopy was performed using a JOEL JEM-100SX operated at 100 kV. Thermogravimetric analysis (TGA) was performed on a TG/DTA6200, SEIKO Instruments, Inc., with the heating rate of $10^\circ\text{C min}^{-1}$ up to 900°C under air.

Octa(3-aminopropyl)octasilsesquioxane Octahydrochloride (1): **1** was prepared according to the previous paper.¹⁰ Amino-propyltriethoxysilane (150 mL, 0.627 mol) and conc. HCl (200 mL) in methanol (3.6 L) produces **1** as a solid after 2 weeks at room temperature. The crude product was obtained after filtration, washing with methanol, and drying. Recrystallization from methanol affords **1** as a white solid. ^1H NMR ((CD_3SO)) δ 8.25 (s, 24H), 2.75 (t, 16H), 1.70 (m, 16H), 0.72 (t, 16H).

Octahydrooctasilsesquioxane (2): **2** was synthesized by the hydrolytic condensation reaction of trichlorosilane, according to the procedure reported before.¹¹ FeCl_3 (anhydrous, 50 g) and conc. HCl (20 mL) were added to the mixture of methanol (40 mL), hexane (350 mL), and toluene (50 mL). A solution of trichlorosilane (20 mL, 0.2 mol) in toluene (150 mL) was then added dropwise over a period of 9 h. after stirring, the upper layer was separated and K_2CO_3 (14 g) and CaCl_2 (10 g) were added. After stirring for 1 day, the mixture was filtered and the filtrate was evaporated under reduced pressure. The obtained product was washed with hexane several times. ^1H NMR (C_6D_6) δ 4.20 (s, 8H).

Preparation of the 1-Protected Gold Nanoparticles: The

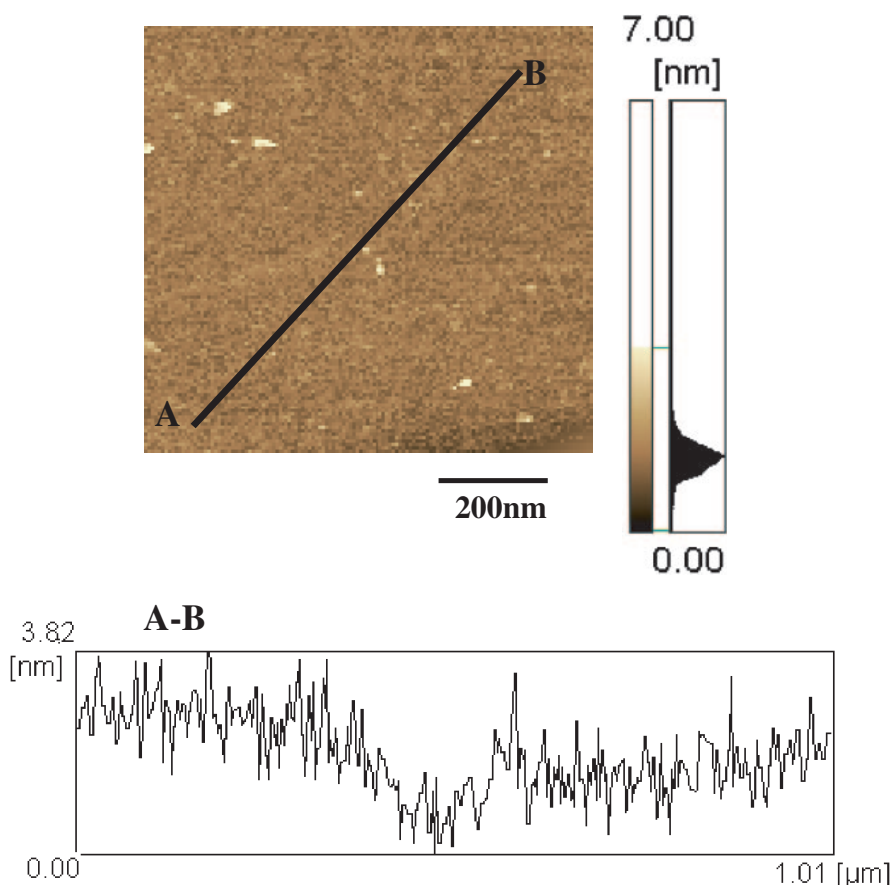


Fig. 4. AFM image of the formation of monolayer of the **1**-protected gold nanoparticles on the glass substrate. The heights profile under the image is the cross section along the line indicated as A–B in the image.

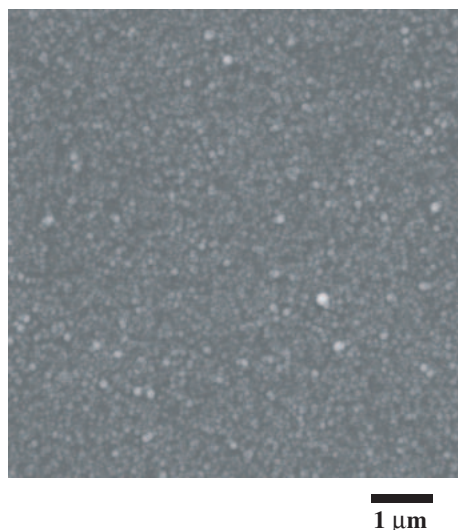


Fig. 5. SEM image of the formation of monolayer of the **1**-protected gold nanoparticles with a diameter of 80 nm on the glass substrate.

typical synthesis procedure is as follows. The aqueous solution (5 mL) of NaBH_4 (5 mg) was added dropwise to 10 mL of an aqueous solution of HAuCl_4 (2.4×10^{-3} M) in the presence of **1** (8.5×10^{-3} M) with stirring. After addition of NaBH_4 , the reaction mixture was allowed to stand for 30 min.

Preparation of Monolayer of Gold Nanoparticles: All glasses used in these preparations were thoroughly cleaned in a bath (75% HCl , 25% HNO_3), rinsed in distilled H_2O , and oven-dried prior to use. Then, the glass was immersed in an aqueous solution of the gold nanoparticles for the prescribed time. After immersion, the glass was washed with H_2O several times to remove extra gold nanoparticles.

We thank Professor T. Fukuda, Dr. Y. Tsujii, and Dr. S. Yamamoto (Institute of Chemical Research, Kyoto University) for the TEM micrographs. We also thank Dr. N. Maruyama (VBL, Kyoto University) for the AFM images.

References

- 1 a) G. Schmid, *Chem. Rev.*, **92**, 1709 (1992). b) G. Schmid, "Clusters and Colloids from Theory to Application," VCH, Weinheim (1992). c) U. Simon, G. Schön, and G. Schmid, *Angew. Chem., Int. Ed. Engl.*, **32**, 250 (1993).
- 2 a) G. Schmid, M. Bäuml, M. Geerkens, I. Heim, C. Osemann, and T. Sawitowski, *Chem. Soc. Rev.*, **28**, 179 (1999). b) C. N. R. Rao, G. U. Kulkarni, P. J. Thomas, and P. P. Edwards, *Chem. Soc. Rev.*, **29**, 27 (2000). c) G. Schmid and L. F. Chi, *Adv. Mater.*, **10**, 515 (1998).
- 3 a) M. Antonietti and C. Göltner, *Angew. Chem., Int. Ed. Engl.*, **36**, 910 (1997). b) M. D. Musick, C. D. Keating, M. H. Keefen, and M. J. Natan, *Chem. Mater.*, **9**, 1499 (1997). c) D. Bethell, M. Brust, D. J. Schiffrin, and C. Kiely, *Electroanal.*

Chem., **409**, 137 (1996). d) A. Doron, E. Katz, and I. Willner, *Langmuir*, **11**, 1313 (1995).

4 a) R. G. Freeman, K. C. Grabar, K. J. Allison, R. M. Bright, J. A. Davis, A. P. Guthrie, M. B. Hommer, M. A. Jackson, P. C. Smith, D. G. Walter, and M. J. Natan, *Science*, **267**, 1629 (1995). b) K. C. Grabar, R. G. Freeman, M. B. Hommer, and M. J. Natan, *Anal. Chem.*, **67**, 735 (1995).

5 a) J. R. Heath, C. M. Knobler, and D. V. Leff, *J. Phys. Chem. B*, **101**, 189 (1997). b) B. O. Dabbousi, C. B. Murray, M. F. Rubner, and M. G. Bawendi, *Chem. Mater.*, **6**, 216 (1994). c) M. Giersig and P. Mulvaney, *Langmuir*, **9**, 3408 (1993). d) T. Teranishi, M. Hosoe, and M. Miyake, *Adv. Mater.*, **9**, 65 (1997).

6 a) J. Schmitt, G. Decher, W. J. Dressick, S. L. Brandow,

R. E. Geer, R. Shashidhar, and J. M. Calvert, *Adv. Mater.*, **9**, 61 (1997). b) N. A. Kotov, I. Dékány, and J. H. Fendler, *J. Phys. Chem.*, **99**, 13065 (1995). c) T. Yonezawa, S. Onoue, and T. Kunitake, *Chem. Lett.*, **1999**, 1061. d) G. Schmid, M. Bäuml, and N. Beyer, *Angew. Chem., Int. Ed.*, **39**, 181 (2000).

7 K. Naka, H. Itoh, and Y. Chujo, *Nano Lett.*, **2**, 1183 (2002).

8 M. Brust, D. Bethell, D. J. Schiffrin, and C. J. Kiely, *Adv. Mater.*, **7**, 795 (1995).

9 M. Sastry, K. S. Mayya, and K. Bandyopadhyay, *Colloids Surf., A* **127**, 221 (1997).

10 F. J. Feher and K. D. Wyndham, *Chem. Commun.*, **1998**, 323.

11 P. A. Agaskar, *Inorg. Chem.*, **30**, 2707 (1991).